Feasibility of Multispectral Airborne Laser Scanning Data for Road Mapping

Kirsi Karila, Leena Matikainen, Eetu Puttonen, and Juha Hyyppä

***Abstract*— Multispectral airborne laser scanning (ALS) data have recently become available. The objective of this letter is to study the feasibility of these data for road mapping—for road detection and road surface classification. The results are compared with the results of traditional aerial ortho images using object-based image analysis and Random Forest classification. The results demonstrate that the multispectral ALS data are feasible for automatic road detection and a significant improvement compared to the use of optical aerial imagery is obtained. In a test using ALS data, 80.5% points representing roads were classified correctly. When aerial images were used, the percentage decreased to 71.6%.**

***Index Terms*— Airborne laser scanning (ALS), image classification, lidar, multispectral, Random Forest (RF), road mapping.**

I. Introduction

THE first commercial multispectral airborne laser scanning (ALS) sensor, Optech Titan, has recently become available. Currently, operational mapping processes are often based on aerial image (AI) data and manual digitizing, and, the automation of the mapping process has proved to be very challenging [1]. Several factors complicate the automated analysis of aerial imagery. These include shadows, tree cover, changing light conditions, and dependence of the reflectance on the illumination and viewing geometry. For active sensors such as ALS the problems of shadows and light conditions can be avoided, and, using multiple channels colored image data can be collected with ALS.

Previous studies have shown the high capability of ALS technology in various mapping applications, including 3-D city modeling [2] and land cover analyses [3]. Conventional ALS with one intensity channel has its main benefits in mapping of elevated objects such as buildings and trees, and mainly classification is done using point cloud metrics. The use of two or more intensity channels can further increase classification accuracy [4], [5], and the first studies with the Optech Titan sensor suggest that multispectral ALS is very promising for also classifying low-level classes such as sealed and unsealed surfaces, roads and low vegetation. Such classifications have been proposed and tested in [6]–[9], but detailed analyses focusing on road mapping are still lacking. Ground-based multispectral lidar has already been found superior to single-band lidar and passive imaging in object classification [4], [10], [11].

A review of impervious surface (roads, buildings) mapping using remote sensing data has been provided in [12]. Automated road mapping from AIs has been discussed in [1], [13], and [14]. A review of urban land cover mapping from ALS has been published in [3]. Automatic road mapping from ALS has been studied in [15] and [16]. Spectral characteristics of road types discussed in [17] and [18] have used hyperspectral images mapping asphalt road conditions.

The objective of this letter is to present the first feasibility study concentrating on road mapping from multispectral ALS. We will focus on detection and classification of paved and gravel roads in a suburban setting. As the map updating is currently often based on aerial ortho images, we will compare the performance of multispectral ALS to the performance of AIs. The research questions addressed are as follows: 1) what is the road detection rate using multispectral ALS data; 2) is it possible to recognize the type of road surface from multispectral ALS data; and 3) which features are useful? We will focus on classification of roads and road-like areas; road vectorization is not included in this letter.

In this letter, the point cloud data are analyzed in a raster format. Some details are lost when point cloud data are converted to the raster format. However, a wide selection of methods is available for raster-based data analysis, and in raster format different data sets can be easily analyzed visually and compared with each other. In particular, comparison to AIs becomes straightforward. In addition to pixel-based image processing methods, object-based methods have become widely available. Object-based methods [19] have been found suitable for classification of data from very high resolution remote sensing sensors because they allow the exploitation of diverse object characteristics instead of single pixel values in the classification process, e.g., mean values, texture, shape, and contextual relationship.

For a large set of input variables, generating classification rules manually is time-consuming, and thus, automatic methods are needed for operational applications. The Random Forest (RF) method creates a large number of classification trees [20]. The advantage of RF is that it handles a large number of input variables and a separate test data set is not necessarily needed as RF estimates an out-of-bag

Manuscript received September 2, 2016; revised October 28, 2016; accepted November 14, 2016. Date of publication January 23, 2017; date of current version February 23, 2017. This work was supported by the Academy of Finland under Grant 295047 (“Integration of large multisource point cloud and image datasets for adaptive map updating”) and Grant 272195 (“Centre of Excellence in Laser Scanning Research”).

The authors are with the Finnish Geospatial Research Institute FGI, National Land Survey of Finland, 02430 Masala, Finland, and also with the Centre of Excellence in Laser Scanning Research, 02430 Masala, Finland (e-mail: Kirsi.Karila@nls.fi).

Digital Object Identifier 10.1109/LGRS.2016.2631261

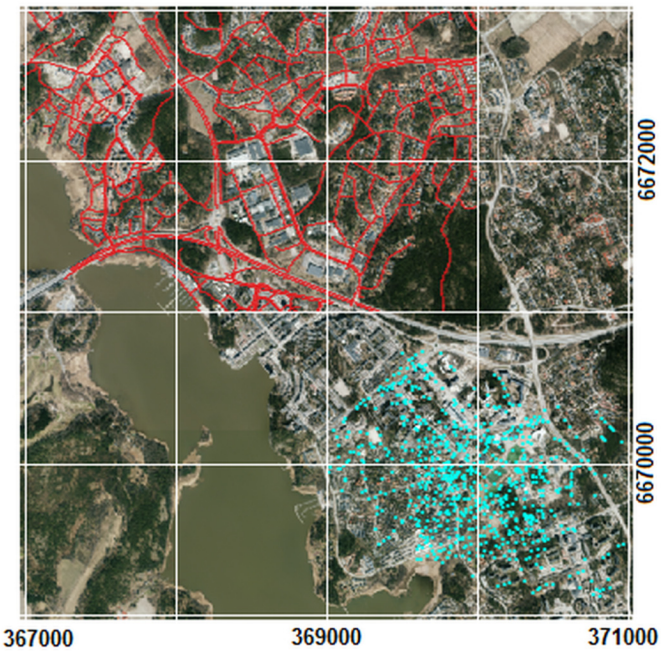

Fig. 1. Study area. (Bottom right) Training points (cyan). (Top left) Test data IIa (red). Coordinates: WGS84/ UTM zone 35N. AI courtesy of NLS, 2013.

error internally during each run. In addition, it estimates which variables are important in the classification (variable importance) [20].

II. Data and Methodology

A. Study Area

The study area is located in Espoo, Southern Finland (60° 9'25 N, 24° 38'0 E). A separate training area is located in Espoonlahti (2.5 km^2), and the test area (6 km^2) comprises of areas of Saunalahti, Kattilalaakso, Tillinmäki (Fig. 1). The area is a suburban area, including dense and sparsely built areas, industrial area, forests, and parks. Roads in the area vary from highways to narrow cycle paths.

B. Remote Sensing Data

The multispectral ALS data were acquired on August 21, 2015 using the Optech Titan sensor, which has three spectral channels; ch1: infrared 1550 nm (∼8 points/m^2 in the study area), ch2: near infrared (NIR) 1064 nm (∼9 points/m^2), and ch3: green 532 nm (∼8 points/m^2). A range correction [21], [22] was applied to avoid lower intensity values near the edges of flight strips. This calibration method takes into account the distance from the scanner to the scanned point in relation to the flying height [23]. The point clouds were rasterized to 20 cm grids representing the average intensity of all pulses, minimum height [minimum digital surface model (MinDSM) in the following discussion] and maximum height (MaxDSM). More details on the data and processing are available in [7] and [24].

For comparison, we used open image data from the National Land Survey (NLS). These data are currently operatively used for map updating in Finland. The AIs used in this letter were acquired on May 3, 2013 using an UltraCamEagle camera. The images have been pan-sharpened and matched to a tonally adjusted model image provided by NLS. The ortho image was produced using NLS digital terrain model (DTM), created from ALS data in 2 m grid. The aerial ortho image has a 50 cm pixel size. According to visual evaluation, the spatial resolution corresponds approximately to the resolution of the multispectral ALS data when the visibility of road features is considered. The AI had four channels: red (ch1), green (ch2), blue (ch3), and NIR regions (ch 4). We also combined height information to the AI using a DSM derived from open NLS single channel ALS data acquired in 2008. The ALS points were rasterized to 1 m grid (MinDSM and MaxDSM).

For the terrain height the NLS 2 m DTM was used for both the multispectral ALS and AIs. It should be noted that a similar terrain model could also be extracted from the multispectral ALS data. However, since the existing DTM has been manually edited, to get a similar result from the multispectral ALS data would require some manual editing, and existing DTM was used.

C. Auxiliary Data

1) Training Data: A total of 367 road training points were selected so that the road surface was visible in both the data sets; the multispectral ALS and the AIs. The points were only placed on roads, not on parking lots or courtyards which may have a similar surface cover. Shadows, road markings, and zebra crossings were not used as road training points. 137 of the points were on gravel roads and 230 on paved roads. The paved roads included mostly asphalt and few different kinds of pavers (e.g., street tiles). For the class "other than road" the training data used in [7] excluding the points presenting paved and gravel surfaces, was used. A total of 66 points were added to outcrop type areas (nonvegetated ground) as the class is easily mixed with roads. In total, there were 330 points in the class "other" including buildings, forest, open vegetated areas, and open natural nonvegetated areas (no parking lots or playgrounds were included).

2) Test/Validation Data: Test data I: The data set consists of 254 land cover ground truth points collected and further classified as gravel surfaces, paved surfaces, and other. 14 points were not on roads, situated mainly on parking lots, a few on playgrounds and courtyards. Error matrices are calculated based on these points.

Test data II: To study road detectability more comprehensively, roads extracted from the NLS Topographic Database were used as validation data. The database included information on the road class (∼width, see Table V) and the road surface (paved or gravel). Test points were created from the road vector data with ca. 10 m interval, resulting in 7346 points (Test data IIa). The data were manually updated for roads with incorrect location or outdated surface information. In addition, some points were excluded in areas that differed significantly in the AI and multispectral ALS data due to different acquisition times. For the validation of the AI + DSM data set, a reduced test set was used because of

TABLE I
ATTRIBUTES DERIVED FOR EACH SEGMENT, QX = X% QUANTILE

	Multispectral ALS	Aerial Image (+ *DSM*)
Mean, Ratio to all, Brightness, Q10,Q25, Q50, Q75, Q90, Q90 - Q10	ch1, ch2, ch3	ch1, ch2, ch3, ch4
Standard deviation	ch1, ch2, ch3, minDSM, maxDSM	ch1, ch2,ch3, ch4, *minDSM, maxDSM*
Ratios of two channels	ch1/ch3, ch1/ch2, ch2/ch3	ch1/ch2, ch1/ch3, ch1/ch4, ch2/ch3, ch2/ch4, ch3/ch4
Normalized difference vegetation index (NDVI)	ch2 & ch3 (pseudo-NDVI; [8])	ch1 & ch4
DSM differences	maxDSM-DTM, minDSM-DTM maxDSM-minDSM	*maxDSM-DTM, minDSM-DTM, maxDSM-minDSM*

the early DSM acquisition date. A total of 3803 points were used for the second comparison (test data IIb).

D. Segmentation

In this letter, the multiresolution segmentation algorithm [25] in the eCognition software (Trimble Germany GmbH, Munich, 2016) was used to divide the images into homogeneous regions, i.e., segments. The multiresolution segmentation algorithm locally minimizes the average heterogeneity of image objects. The scale parameter (related to image object size) is an abstract term that determines the maximum allowed heterogeneity for the resulting image objects. The object homogeneity (minimized heterogeneity) is a combination of color and shape, and further, shape is a combination of smoothness and compactness.

The three intensity channels were used as input data in the segmentation process of the multispectral ALS data. The segmentation parameters for the multispectral ALS intensity data were scale 2, shape 0.01 and compactness 0.05. For the AIs the parameters were scale 10, shape 0.5, and compactness 0.9. The choice of parameters was based on a visual analysis of the segment size and shape.

After the segmentation, the segment attributes were calculated. Several multispectral features were included since it was assumed that they are important in separating targets on the ground level (e.g., roads). Basic geometric features were also included. The attributes extracted for each data set are listed in Table I.

E. Classification

To study first the road detection rate only, the classification test was divided into two parts: 1) road detection: road/other land cover and 2) road surface classification: paved/gravel. Road surface was classified only for the segments classified as road. Three data sets were studied: 1) multispectral ALS; 2) AI; and 3) AI + DSM from one-channel ALS.

For each training point, the corresponding segment is selected. The segments and attributes are imported to MATLAB 2015b (The MathWorks Inc, Natick, MA, USA). The RF models are trained using MATLAB'S RF implementation (fitensemble with bagging) included in its Statistics and Machine Learning Toolbox [26]. A total of 1,000 classification trees were used for the classification. From the training data out-of-bag classification error is estimated by leaving part of the training data for validation. In addition, the importance of each predictor (segment attribute) is estimated.

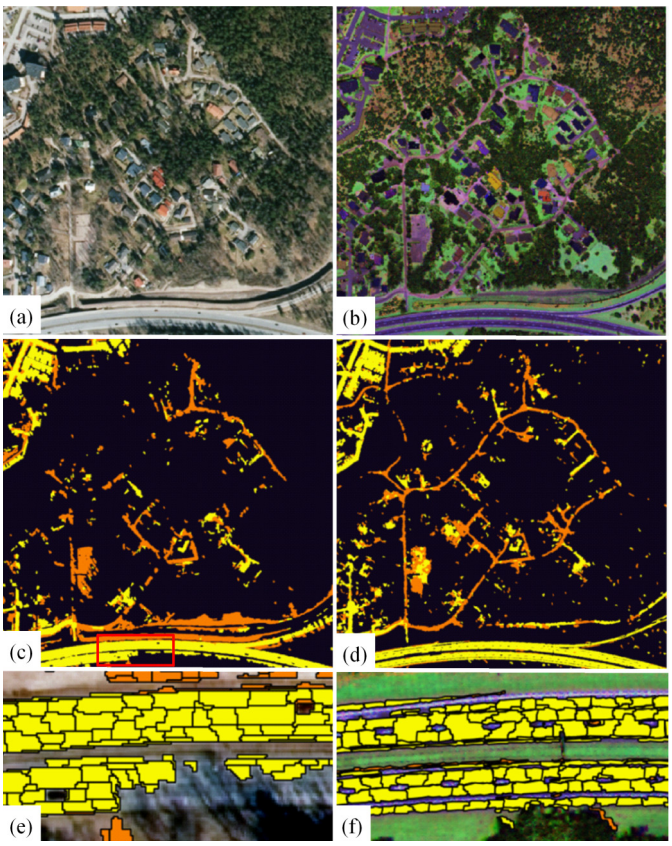

Fig. 2. (a) AI. (b) Rasterized ALS intensity data (R:ch1,G:ch2, B:ch3). (c) AI classification: detected roads in yellow (asphalt) and orange (gravel). (d) Multispectral ALS classification. (e) Close-up view [the red rectangle in (c)] of the AI results; only segments classified as road are shown. Two cars and shadows can be seen in the AI not classified as road. (Top) AI of newly built noise barrier without vegetation classified as gravel road. (f) MS-ALS result: road markings cause omission errors. AI courtesy of NLS, 2013.

TABLE II
OUT-OF-BAG CLASSIFICATION ERROR FOR THE TRAINING DATA

	MS-ALS	AI	AI + DSM
Road detection	2.6 %	4.5 %	3.9 %
Surface classification	4.2 %	7.8 %	7.8 %

III. RESULTS

The RF model was trained using the training points, and, during the training out-of-bag error and predictor importance was estimated for the training data. The out-of-bag classification errors are listed in Table II. An example of the classification results is presented in Fig. 2. Fig. 2 clearly demonstrates the feasibility of multispectral ALS intensities to detect roads compared to aerial imaging.

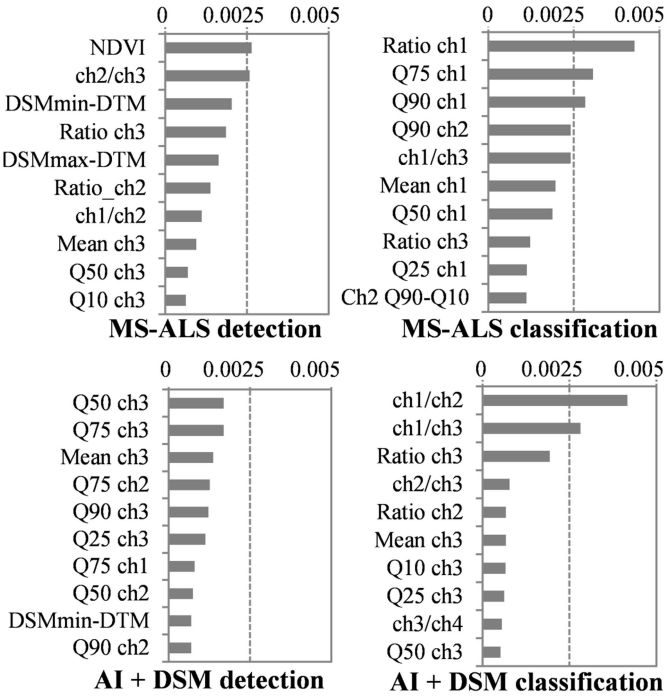

Fig. 3. Feature importance for ten most important features in RF classification of different data sets.

TABLE III
ERROR MATRICES FOR (TOP) MULTISPECTRAL ALS AND (BOTTOM) AI USING TEST DATA I

Ground truth (Test data I)					
MS-ALS result	Other	Gravel	Paved	Total	Correctness
Other	186	0	6	192	96.9 %
Gravel	3	4	1	8	50.0 %
Paved	4	1	49	54	90.7 %
Total	193	5	56	254	
Completeness	96.4 %	80.0 %	87.5 %		
Overall accuracy: **94.1 %**				Kappa: **0.844**	
AI result	Other	Gravel	Paved	Total	Correctness
Other	189	3	12	204	92.6 %
Gravel	3	2	3	8	25.0 %
Paved	1	0	41	42	97.6 %
Total	193	5	56	254	
Completeness	97.9 %	40.0 %	73.2 %		
Overall accuracy: **91.3 %**				Kappa**: 0.754**	

The most important features for road detection in the multispectral ALS data and AIs + DSM data are presented in Fig. 3.

The error matrix (Table III) was calculated based on Test data set I. The overall accuracy for classification of gravel, paved, and other was 94.1% for the multispectral ALS, 91.3 % for the AI, and for AI + DSM 91.7 % (class change of one point in comparison to AI alone).

To study the detectability of realistic roads with shadows and vegetation covering parts of the road, test data IIa from the topographic database was used. The results are reported for the test area in Table IV. The road surface classification was carried out for the segments classified as roads. The road detection results based on the road class in the topographic database are listed in Table V.

TABLE IV
TEST DATA IIA DETECTION RATES (%) AND CLASSIFIED CORRECTLY (%)

	# of points	Detection		Classification	
		MS-ALS	AI	MS-ALS	AI
Gravel	1848	63.6 %	50.6 %	90.0 %	79.6 %
Paved	5498	86.2 %	78.6 %	94.6 %	86.0 %
Total	**7346**	**80.5 %**	**71.6 %**	**93.7 %**	**84.8 %**

TABLE V
DETECTION RATES FOR THE ROAD CLASSES (TEST DATA IIA)

Road class	# of points	MS-ALS %	AI %
Expressway	444	78.6 %	84.2 %
Road, 2 lanes, 5 - 8 m	830	85.8 %	83.0 %
Road, 1 lane, 3 - 5 m	3058	88.8 %	77.6 %
Cycle way / Driveway < 3 m	3014	70.9 %	60.5 %

To validate the AI + DSM data set, the smaller point set IIb was used. For comparison, the other data sets were also validated using this subset of points. The percentage of roads classified as roads was 78.3 % for the multispectral ALS, 68.1% for the AI, and 69.3 % for the AI + DSM data set.

IV. DISCUSSION AND CONCLUSION

There is a significant difference between the out-of-bag classification accuracy (Table II) and the validation accuracy (Table IV). The reason is that the out-of-bag estimate is based on the training points that where selected to present the road surface (road surface visible, no shadows, vehicles, etc.). Based on the out-of-bag accuracies the multispectral ALS data are slightly better in road detection and road surface classification than the AIs. The test data IIa shows a larger difference in the road detection accuracy (80.5 % road detected in multispectral ALS and 71.6 % in AIs). Test data I included paved and gravel surfaces other than roads and also a very small number of gravel road points, which makes the comparison to test data II and training data difficult.

Leaves were on trees when the multispectral ALS data was acquired. The AI was acquired in leaves-off conditions. Therefore, the performance of multispectral ALS data in comparison to AIs for road detection is likely to improve when leaf-off ALS data is available. An analysis approach avoiding tree points and exploiting ground points under trees might also lead to some improvement.

Omission errors in road detection from the ALS data were caused by trees (direct blocking), road surface markings, vehicles on the roads, and road reflectance being different from the training data. Parking lots, courtyards, construction sites, and playgrounds were classified into the same class as roads with the same surface cover. Whether this is a problem depends on the end user of the data. For the AIs shadows were also causing classification errors.

Differences in detection rate of gravel and paved roads (Table IV) are likely caused by the fact that 73% of the gravel roads are narrow cycle ways, and 14 % are driveways under 3 m. Therefore, the detection rates for gravel are lower than for asphalt in both the data sets.

In many cases gravel, new and old asphalt, and different pavers can be separated in the multispectral ALS data visually. In addition, the road surface classification results show slightly better accuracy for the ALS. Higher resolution AIs might perform better; however, for higher resolution AIs the same problems with light conditions and shadows would exist. It is possible to carry out advanced radiometric corrections on AIs to improve the results, however, it is not as simple to perform as the intensity calibration of ALS data. In addition, the AI was acquired two years earlier than the multispectral ALS data. Therefore, for few roads the surface may not be the same in multispectral ALS and AI data in the Test data II.

The analysis based on the road class is hindered by different number of points per class (Table V) and uncertainty in the class definition. However, a comparison of classes with most points, "road 3–5 m" and "cycle way" gives an idea of how the road width affects the road detection (89 % versus 71 % classified as road). It can also be noted that the express way has notably lower accuracy than some smaller roads for the multispectral ALS data. A more detailed examination showed that many of the expressway points are located on the centerline markings. In the multispectral ALS data, the lane markings are not classified as road. The ALS data had a smaller pixel size and different spectral channels than the AIs resulting in paintings as separate segments. For the AIs the paintings were mostly included in the road segments.

Different acquisition times and varying reflectance of the AIs are a real problem for automated image interpretation methods. The multispectral ALS intensity should have better consistency between image acquisitions for stable targets such as roads. Of course, changes in target properties, e.g., wetness will have an effect on the data.

The scope of this letter was not to extract complete road network. Some of the classification problems (e.g., road markings and vehicles) could be solved by doing additional pre- or postprocessing steps on the data and the results. In any case, multispectral ALS data are very promising input data for more advanced road detection algorithms.

ACKNOWLEDGMENT

The authors would like to thank the intensity calibration of the multispectral ALS data performed by P. Litkey and the multispectral ALS data acquired in cooperation with TerraTec Oy, Helsinki, Finland.

REFERENCES

[1] H. Mayer, S. Hinz, U. Bacher, and E. Baltsavias, "A test of automatic road extraction approaches," *Int. Arch. Photogramm. Remote Sens. Spatial Inf. Sci.*, vol. 36, no. 3, pp. 209–214, 2006.

[2] N. Haala and M. Kada, "An update on automatic 3D building reconstruction," *ISPRS J. Photogramm. Remote Sens.*, vol. 65, no. 6, pp. 570–580, 2010.

[3] W. Y. Yan, A. Shaker, and N. El-Ashmawy, "Urban land cover classification using airborne LiDAR data: A review," *Remote Sens. Environ.*, vol. 158, pp. 295–310, Mar. 2015.

[4] J. Vauhkonen *et al.*, "Classification of spruce and pine trees using active hyperspectral LiDAR," *IEEE Geosci. Remote Sens. Lett.*, vol. 10, no. 5, pp. 1138–1141, Sep. 2013.

[5] C.-K. Wang, Y.-H. Tseng, and H.-J. Chu, "Airborne dual-wavelength LiDAR data for classifying land cover," *Remote Sens.*, vol. 6, no. 1, pp. 700–715, 2014.

[6] K. Bakuła, P. Kupidura, and Ł. Jełowicki, "Testing of land cover classification from multispectral airborne laser scanning data," *Int. Arch. Photogramm. Remote Sens. Spatial Inf. Sci.*, vol. 7, pp. 161–169, Jun. 2016.

[7] L. Matikainen, J. Hyyppä, and P. Litkey, "Multispectral airborne laser scanning for automated map updating," *Int. Arch. Photogramm. Remote Sens. Spatial Inf. Sci.*, vol. 3, pp. 323–330, Jun. 2016.

[8] V. Wichmann, M. Bremer, J. Lindenberger, M. Rutzinger, C. Georges, and F. Petrini-Monteferri, "Evaluating the potential of multispectral airborne LiDAR for topographic mapping and land cover classification," in *Proc. ISPRS Ann. Photogramm. Remote Sens. Spatial Inf. Sci.*, vol. II-3/W5. Aug. 2015, pp. 113–119.

[9] X. Zou, G. Zhao, J. Li, Y. Yang, and Y. Fang, "3D land cover classification based on multispectral LiDAR point clouds," *Int. Arch. Photogramm. Remote Sens. Spatial Inf. Sci.*, XLI-B1, vol. 41, no. B1, pp. 741–747, 2016.

[10] E. Puttonen, A. Jaakkola, P. Litkey, and J. Hyyppä, "Tree classification with fused mobile laser scanning and hyperspectral data," *Sensors*, vol. 11, no. 5, pp. 5158–5182, 2011.

[11] W. Gong *et al.*, "Investigating the potential of using the spatial and spectral information of multispectral LiDAR for object classification," *Sensors*, vol. 15, no. 9, pp. 21989–22002, 2015.

[12] Q. Weng, "Remote sensing of impervious surfaces in the urban areas: Requirements, methods, and trends," *Remote Sens. Environ.*, vol. 117, no. 15, pp. 34–49, Feb. 2012.

[13] E. Baltavias and C. Zhang, "Automated updating of road databases from aerial images," *Int. J. Appl. Earth Observ. Geoinf.*, vol. 6, no. 3, pp. 199–213, 2005.

[14] C. Zhang, E. Baltsavias, and A. Gruen "Updating of cartographic road databases by image analysis," Ph.D. dissertation, Inst. Geodesy Photogramm., ETH Zürich, Zürich, Switzerland, 2003.

[15] S. Clode, F. Rottensteiner, P. Kootsookos, and E. Zelniker, "Detection and vectorization of roads from LiDAR data," *Photogramm. Eng. Remote Sens.*, vol. 73, no. 5, pp. 517–535, May 2007.

[16] F. Samadzadegan, M. Hahn, and B. Bigdeli, "Automatic road extraction from LiDAR data based on classifier fusion," in *Proc. Joint Urban Remote Sens. Event*, Shanghai, China, May 2009, pp. 1–6.

[17] C. Andreou, V. Karathanassi, and P. Kolokoussis, "Investigation of hyperspectral remote sensing for mapping asphalt road conditions," *Int. J. Remote Sens.*, vol. 32, no. 21, pp. 6315–6333, 2011.

[18] M. Herold, D. A. Roberts, M. E. Gardner, and P. E. Dennison, "Spectrometry for urban area remote sensing—Development and analysis of a spectral library from 350 to 2400 nm," *Remote Sens. Environ.*, vol. 91, no. 3, pp. 304–319, 2004.

[19] T. Blaschke, "Object based image analysis for remote sensing," *ISPRS J. Photogramm. Remote Sens.*, vol. 65, no. 1, pp. 2–16, Jan. 2010.

[20] L. Breiman, "Random forests," *Mach. Learn.*, vol. 45, no. 1, pp. 5–32, 2001.

[21] E. Ahokas, S. Kaasalainen, J. Hyyppä, and J. Suomalainen, "Calibration of the Optech ALTM 3100 laser scanner intensity data using brightness targets," *Int. Arch. Photogramm. Remote Sens. Spatial Inf. Sci*, vol. 36, pp. 1–6, May 2006.

[22] B. Höfle and N. Pfeifer, "Correction of laser scanning intensity data: Data and model-driven approaches," *ISPRS J. Photogramm. Remote Sens.*, vol. 62, no. 6, pp. 415–433, Dec. 2007.

[23] I. Korpela, H. O. Ørka, V. Heikkinen, T. Tokola, and J. Hyyppä, "Range and AGC normalization in airborne discrete-return LiDAR intensity data for forest canopies," *ISPRS J. Photogramm. Remote Sens.*, vol. 65, no. 4, pp. 369–379, 2010.

[24] E. Ahokas *et al.*, "Towards automatic single-sensor mapping by multispectral airborne laser scanning," *Int. Arch. Photogramm. Remote Sens. Spatial Inf. Sci.*, vol. 41, pp. 155–162, Jul. 2016.

[25] M. Baatz and A. Schäpe, "Multiresolution Segmentation: An optimization approach for high quality multi-scale image segmentation," in *Angewandte Geographische Informationsverarbeitung XII. Beiträge Zum AGIT-Symposium Salzburg 2000*, J. Strobl, T. Blaschke, and G. Griesebner, Eds. Heidelberg, Germany: Wichmann, 2000, pp. 12–23.

[26] *Online Documentation for Statistics and Machine Learning Toolbox, Version R2015b*, MathWorks, Inc., Natick, MA, USA, 2016.